

Electronic noise and impedance field of submicron n^+nn^+ InP diode generators

V Gružinskis†, E Starikov†, P Shiktorov†, R Gricius†, V Mitin‡,
L Reggiani§ and L Varani¶¶

† Semiconductor Physics Institute, A Goštauto 11, 2600 Vilnius, Lithuania

‡ Department of Electrical and Computer Engineering, Wayne State University,
Detroit, MI 48202, USA

§ Dipartimento di Fisica ed Istituto Nazionale di Fisica della Materia, Università di
Modena, Via Campi 213/A, 41100 Modena, Italy

¶ Centre d'Electronique de Montpellier, Université Montpellier II, 34095 Montpellier
Cedex 5, France

Received 31 May 1994, accepted for publication 7 July 1994

Abstract. We investigate the electronic noise and impedance field of submicron n^+nn^+ diode generators when loaded by an external resistance in the framework of a Monte Carlo and a hydrodynamic simulative approach. We observe a long-time oscillation of the correlation function of the voltage drop fluctuations between the resistor terminals. The oscillations are in turn responsible for a peak in the noise power-spectrum which is caused by the spontaneous formation of electron accumulation layers. The drift of these layers through the n-region is monitored for biasing conditions above threshold for microwave generation. The frequency of the noise peak is shown to correspond to the highest generation frequency for the given load resistance. The noise power-spectra calculated for three different values of the load resistance are used to obtain the small-signal and noise characteristics of the intrinsic unloaded diode. The parallel hydrodynamic calculation of the diode impedance spectrum is found to compare well with the results obtained from the noise analysis of the Monte Carlo simulation.

1. Introduction

The determination of the small-signal AC characteristics and noise spectra is of basic importance in understanding the behaviour and providing figures of merit for microwave generators. From a fundamental point of view, the time and frequency behaviour of fluctuations reflect both the dynamic and random features of the hot-carrier system and, as such, can be used for a detailed investigation of the physical processes that are responsible for the device performance [1, 2]. From an applied point of view, noise characteristics are important since they determine the lower limit of device sensitivity, indicate the onset of generation processes, etc [3, 4]. Furthermore, noise reduction remains one of the main problems to be faced by device designers.

The aim of this work is to provide a theoretical analysis of the hot-carrier noise in submicron n^+nn^+ diodes under biasing conditions for which microwave power generation associated with velocity overshoot and electron valley transfer is possible. In so doing,

useful relationships between fluctuations and small-signal kinetic coefficients are also investigated. The paper is organized as follows. Section 2 reports the analytical expressions and properties of the physical quantities of interest. The results of the simulations, which are performed for the case of structures made by InP, are displayed and discussed in section 3. The main conclusions are summarized in section 4.

2. Theory

The Monte Carlo particle (MCP) method is the most appropriate technique for investigating hot-carrier noise since it allows the appropriate correlation functions to be calculated in a natural way, by using a time-averaging over a multi-particle history simulated during a sufficiently long time interval. As a rule, MCP is used to calculate spectral densities of either current or voltage noise [2, 5]. These noise operations correspond to the idealized condition when either the voltage applied to the diode, U_d , or the total current per unit area as measured in the outside short circuit, j , is kept constant in time. Current noise operation occurs when the diode resistance R_d is much greater than the external load

¶¶ On leave from Dipartimento di Fisica ed Istituto Nazionale di Fisica della Materia, Università di Modena, Via Campi 213/A, 41100 Modena, Italy.

resistance R connected in series with the diode. Voltage noise operation occurs in the opposite case. To evaluate the electronic noise of the diode in the intermediate cases, we propose to study the voltage fluctuations at the terminals of the noiseless load resistance. To this purpose, the correlation function of the fluctuations of the voltage drop $U_R(t)$ on the load resistance, $C_U(t)$, is calculated as

$$C_U(t) = \frac{1}{T} \int_0^T \delta U_R(t') \delta U_R(t' + t) dt' \quad (1)$$

where T is the averaging time, $\delta U_R(t) = R \delta j(t)$ is the fluctuation of U_R caused by the fluctuation of the total current, $\delta j(t)$, which accounts for both the conduction and displacement currents. Then, the noise power spectral density $P_n(f)$ extracted from the load resistance in the frequency bandwidth Δf around the frequency f is calculated in the standard way as

$$P_n(f) = \frac{4}{R} \int_0^\infty C_U(t) \cos(2\pi f t) dt. \quad (2)$$

The advantage of this procedure is that $P_n(f)$ is an invariant of the whole circuit and, by varying R and keeping the average voltage applied to the diode U_d constant in time, one can perform a continuous investigation of the diode noise from the current to the voltage noise operation. Moreover, by assuming a linear regime of generation, one can relate $P_n(f)$ to the small-signal and noise characteristics of the intrinsic diode through [1]

$$P_n(f) = \frac{S_U(f) R}{|Z(f) + R|^2} \quad (3)$$

where $S_U(f)$ is the spectral density of voltage fluctuations of the unloaded diode calculated under constant-current operation and $Z(f)$ is the complex small-signal impedance of the diode. One can treat equation (3) as an equation that contains three unknown functions, namely $S_U(f)$ and the real and imaginary parts of the small-signal impedance, $\text{Re}[Z(f)]$ and $\text{Im}[Z(f)]$ respectively. Therefore, by using the $P_n(f)$ obtained for three different values of R , one can obtain from equation (3) the frequency dependence of $S_U(f)$, $\text{Re}[Z(f)]$ and $\text{Im}[Z(f)]$ of the unloaded diode. Accordingly, for $\text{Re}[Z(f)]$ one obtains

$$\begin{aligned} \text{Re}[Z(f)] \\ = \frac{a_1 R_1^2(a_2 - a_3) + a_2 R_2^2(a_3 - a_1) + a_3 R_3^2(a_1 - a_2)}{-2[a_1 R_1(a_2 - a_3) + a_2 R_2(a_3 - a_1) + a_3 R_3(a_1 - a_2)]} \end{aligned} \quad (4)$$

where $a_i = P_n(f, R_i)/R_i$. It should be remarked that all terms of the type $(a_i - a_j)$ in equation (4) are of the same order of magnitude and can assume positive or negative values. Therefore, the spectra of $P_n(f)$ at different R must be calculated with a sufficiently high accuracy, the best results being obtained when the R_i differ considerably one from another. An equation similar to (4) is obtained for $\{\text{Im}[Z(f)]\}^2$. In evaluating

the square root to obtain $\text{Im}[Z(f)]$ one must take the minus sign since only the negative values of $\text{Im}[Z(f)]$ correspond to a stable operation point at the given bias, i.e. self-oscillations are absent [6]. Then, the direct substitution of the obtained $Z(f)$ into equation (3) gives the $S_U(f)$. By using the values of $Z(f)$ and $S_U(f)$ so obtained, one can calculate the corresponding spectral density of the current fluctuations under constant-voltage operation, $S_j(f)$, from the well known relationship [1]

$$S_j(f) = \frac{S_U(f)}{|Z(f)|^2}. \quad (5)$$

To verify the above procedure and to better clarify the physical origin of the hot-carrier noise, we have also calculated $Z(f)$ for the same diode by using a closed hydrodynamic (HD) approach that we have previously developed [7]. The details of the MCP and HD techniques used in our calculations can be found in reference [8].

3. Results and discussion

The following parameters for the n^+nn^+ InP diode are chosen in the present simulation: the length of the n-region is $0.6 \mu\text{m}$, and the doping concentration in the n- and n^+ -regions is $3 \times 10^{16} \text{ cm}^{-3}$ and 10^{18} cm^{-3} respectively. The current-voltage characteristic of this structure does not exhibit any region with a static negative differential resistivity (NDR). However, there exists a dynamic NDR in the frequency region $f \equiv 160\text{--}400 \text{ GHz}$ where $\text{Re}[Z(f)]$ is negative. The voltage threshold for the presence of a dynamic NDR is $U_{th} = 1.3 \text{ V}$.

Quite different behaviours of the noise power spectral density are obtained for values of the applied voltages below and above the NDR threshold U_{th} . Below the threshold, when $\text{Re}[Z(f)]$ is positive at all frequencies, $P_n(f)$ exhibits the expected Lorentzian shape with two additional peaks at the frequencies corresponding to the plasma oscillations characteristic of the n- and n^+ -regions. Above the threshold, $P_n(f)$ exhibits a huge peak whose amplitude and position depend on the value of R .

Figure 1 shows the correlation functions of the voltage fluctuations at the load resistance terminals calculated for different values of R : (a) 2×10^{-10} , (b) 4×10^{-9} and (c) $2 \times 10^{-8} \Omega\text{m}^2$. Here the voltage applied to the diode is $U_d = 3 \text{ V}$, which is considerably above the threshold value, and remains the same for all the curves. Two types of oscillations of $C_U(t)$ are observed. On a short time scale one can detect higher frequency oscillations which are connected with the plasma frequency of the n^+ contacts. These oscillations are responsible for the appearance of the resonant peak in $P_n(f)$ near $f = 8 \text{ THz}$. On a long time scale one can detect a high-frequency oscillation caused by the spontaneous formation of electron accumulation layers and their subsequent drift through the n-region. The layers' formation is related to the spatial overshoot of the drift velocity due to an electron transfer to upper

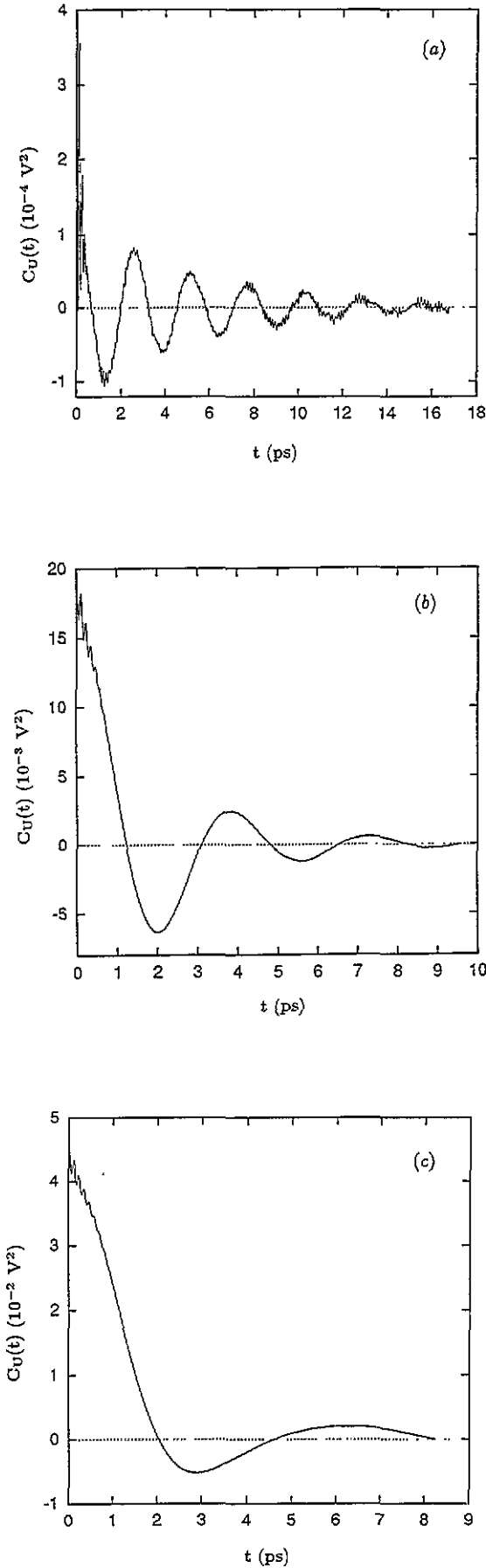


Figure 1. Time dependences of the correlation functions of the voltage drop fluctuations at the terminals of the load resistance calculated by the MCP simulation for $U_d = 3.0 \text{ V}$ at different values of the load resistance: (a) 2×10^{-10} , (b) 4×10^{-9} and (c) $2 \times 10^{-8} \Omega \text{ m}^2$.

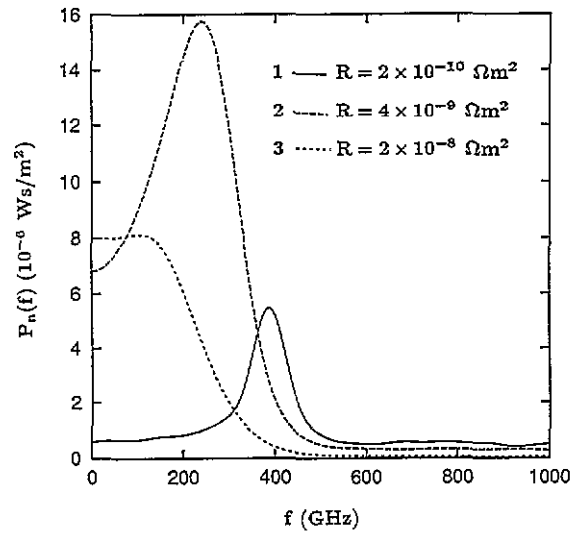


Figure 2. Noise power spectral densities $P_n(f)$ obtained by Fourier transforming the correlation functions of figure 1. Curves 1, 2 and 3 refer to $R = 2 \times 10^{-10}$, 4×10^{-9} and $2 \times 10^{-8} \Omega \text{ m}^2$.

valleys, and it usually takes place in the region where the local drift velocity exhibits the maximum negative slope [9]. The oscillation frequency is determined by the average transit time that is necessary for the layer to be formed and to cross the diode. The variation of the time dependence of $C_U(t)$ with R shows a continuous transition from voltage- to current-driven operation. When the load resistance is small enough, pronounced oscillations of both types (plasma and transit-time) are detected (see figure 1(a)). An increase of R leads to a damping of both oscillations (see figure 1(b)). Under the condition close to current-driven operation, all current oscillations are effectively damped due to the influence of a very high load resistance (see figure 1(c)).

Figure 2 shows the noise power spectral densities obtained by Fourier transforming the correlation functions reported in figure 1. The variation of $P_n(f)$ with R reflects a continuous transition from the current to the voltage noise operation. Indeed, the most pronounced peak of $P_n(f)$ is observed when R is relatively small, i.e. under the conditions close to the current noise operation. Such a peak is similar to that of the spectral density of current fluctuations as obtained for an unloaded diode under constant-voltage operation [10]. This peak is caused by the spontaneous formation of electron accumulation layers and their subsequent drift through the n-region. The peak frequency f_0 is determined by the average transit time of the layer. Under conditions close to voltage noise operation, all current oscillations are effectively damped. Therefore, the peak of $P_n(f)$ practically disappears for high values of R (see curve 3), and the shape of the frequency dependence of $P_n(f)$ becomes very similar to the spectral behaviour of the voltage fluctuations of the unloaded diode calculated under constant-current operation [10].

As seen in figure 2, the peak frequency f_0 shifts to lower values as R increases. To explain such a red-shift, we recall that in accordance with equation (3) this behaviour must result from a combined action

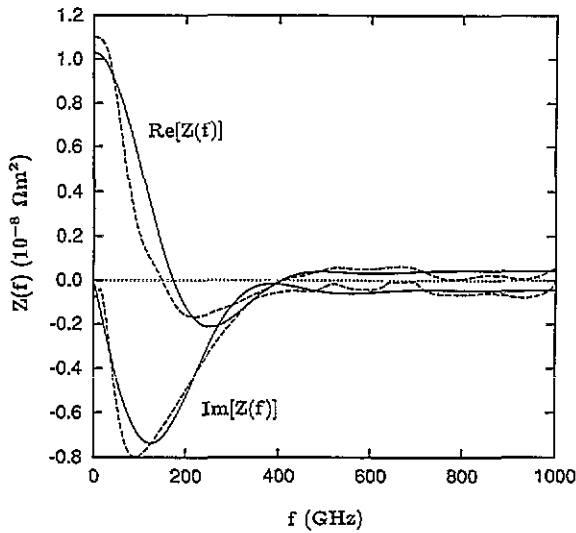


Figure 3. Frequency dependences of the real and imaginary parts of the small-signal impedance as obtained from the HD and MCP approaches (full and broken curves respectively).

of the frequency behaviour of $S_U(f)$, $\text{Re}[Z(f)]$ and $\text{Im}[Z(f)]$. To obtain the spectral behaviour of the above quantities, one can use equations (3)–(5) and the $P_n(f)$ spectra calculated from the MCP method at three different values of R . The results for $\text{Re}[Z(f)]$ and $\text{Im}[Z(f)]$, as obtained through this procedure by using the noise power spectra shown in figure 2, are presented in figure 3 as the broken curves. For the sake of comparison, in the same figure we have also reported as full curves the results obtained with the HD approach. From the good agreement found here between the different approaches we conclude that the proposed procedure can be used for an indirect calculation of the small-signal impedance, provided the $P_n(f)$ spectra are calculated with a sufficiently high accuracy.

Figure 4 reports the intrinsic spectral density of the voltage fluctuations of the diode itself calculated from equation (3) using for $Z(f)$ the values obtained from the MCP simulations. The general shape of this spectrum is in good qualitative agreement with the spectrum obtained by a direct MCP simulation [10]. For comparison, figure 4 also shows the spectral density of the voltage fluctuations obtained by the HD approach for the same diode using the procedure developed in reference [10].

Let us now come back to the discussion of the red-shift of $P_n(f)$ with increasing R (see figure 2). As follows from figure 4, the frequency dependence of $S_U(f)$ does not exhibit any resonant behaviour; therefore, according to equation (3), the peak of $P_n(f)$ must be caused by a resonant behaviour of the denominator of equation (3). Figure 5 shows the frequency dependence of $\text{Re}[Z(f)]$ calculated for the same diode at $U_d = 3$ V (full curve). In general, a small signal is amplified when $\text{Re}[Z(f)]$ is negative. For the case considered here, this condition is fulfilled in the range of frequencies $f \approx 160$ –400 GHz. For values of U_d above the threshold, i.e. when $\text{Re}[Z(f)] < 0$ within a certain frequency range, due to the spontaneous formation of accumulation layers, the generation process

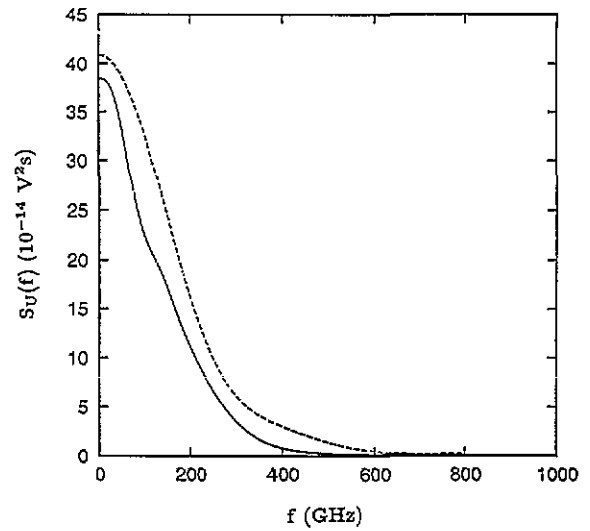


Figure 4. Frequency dependence of the spectral density of voltage fluctuations at the diode terminals calculated by the MCP and HD approaches (full and broken curves respectively).

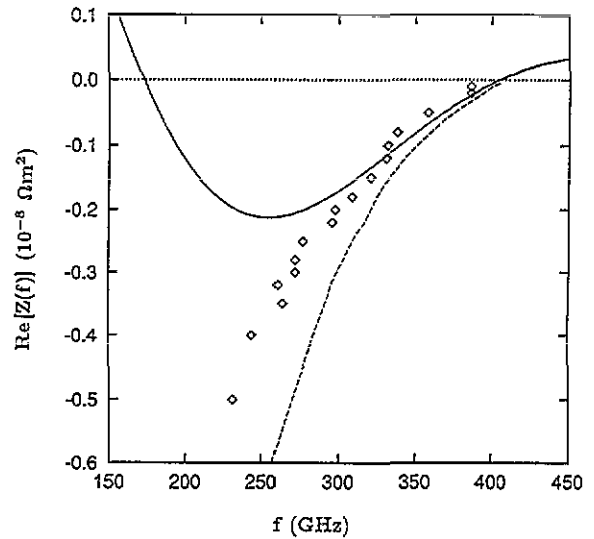


Figure 5. Real part of the impedance spectrum of the unloaded diode in the frequency range of the dynamic NDR calculated by the HD approach (full curve). The broken curve and points correspond to the dependence of the peak frequency on the load resistance for $U_d = 3$ V as obtained from the HD and MCP approaches respectively.

is always present in the structure even in the absence of a resonant circuit. A stable regime of microwave power generation is achieved when the total resistance of the circuit, $R + \text{Re}[Z(f)]$, is equal to zero. Accordingly, the generation frequency f_0 must satisfy the condition $\text{Re}[Z(f_0)] = -R$. In the case of an idealized circuit, this means that for current noise (i.e. when $R = 0$) the frequency of spontaneous generation must coincide with either the left or the right point at which $\text{Re}[Z(f)]$ crosses the zero axis. The right point corresponds to the shortest transit time, when the accumulation layer is formed near the point where the negative slope of the drift velocity takes its maximum value. The left point corresponds to the longest transit time, when the layer is formed at the beginning of the active zone of the diode, just after the maximum of the velocity overshoot. Since

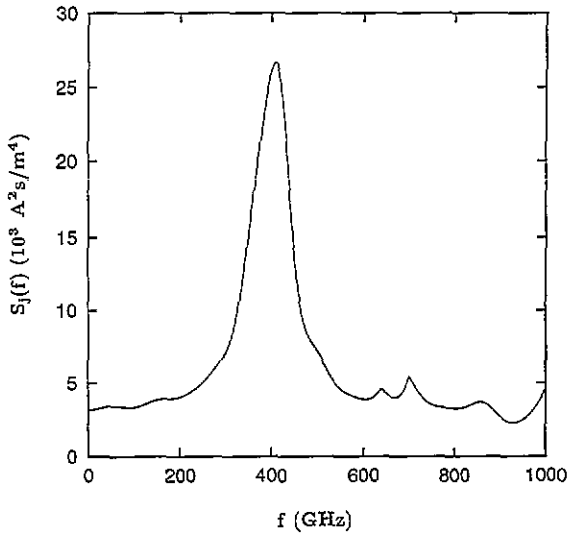


Figure 6. Frequency dependence of the spectral density of current fluctuations of the unloaded diode.

the conditions for layer growth are found to be much more favourable in the former case than in the latter one, the spontaneous generation of the unloaded diode occurs at the maximum frequency [6]. This case corresponds to the current noise shown in figure 6. An increase of R is equivalent to a shift of the x -axis in figure 5 downward with respect to the zero level; therefore, the frequency of spontaneous generation must initially follow the right (high-frequency) wing of $\text{Re}[Z(f)]$.

When R remains less than the maximum absolute value of the negative $\text{Re}[Z(f)]$, R_{\max} , the generation frequency must coincide with the right point at which the horizontal line $-R$ crosses the $\text{Re}[Z(f)]$ curve. The inclusion of $\text{Im}[Z(f)]$, which is small in this frequency range (see figure 3), can slightly modify this relation in accordance with equation (3). When R becomes greater than R_{\max} the amplification condition fails. However, a spontaneous formation of the accumulation layers still takes place. Therefore, the frequency of this generation must satisfy a condition of minimum damping (i.e. must be near the frequency corresponding to the minimum of the $\text{Re}[Z(f)]$ curve) in which the total resistance of the circuit reaches a minimum positive value so that the resonant behaviour of the denominator of equation (3) still takes place. When R becomes much greater than $\text{Re}[Z(f)]$, any resonant behaviour of the diode disappears together with the process of spontaneous generation. The peak of $P_n(f)$ is in this case of a non-resonant nature, being the result of a competition among the frequency dependence of $S_U(f)$, $\text{Re}[Z(f)]$ and $\text{Im}[Z(f)]$ (see figures 3 and 4).

To verify this expectation, the dependence of the peak frequency f_0 on R , as obtained from the results of the MCP calculations, is presented in figure 5 by dots with coordinates $(f_0, -R)$. One can see that the dots get closer to the high-frequency side of the impedance spectrum. When R becomes greater than R_{\max} , in the dynamic NDR region the coordinates $(f_0, -R)$ depart from the $\text{Re}[Z(f)]$ behaviour, simply describing a shift of the $P_n(f)$ maximum to the lower frequency range. For comparison, figure 5 also reports as a broken

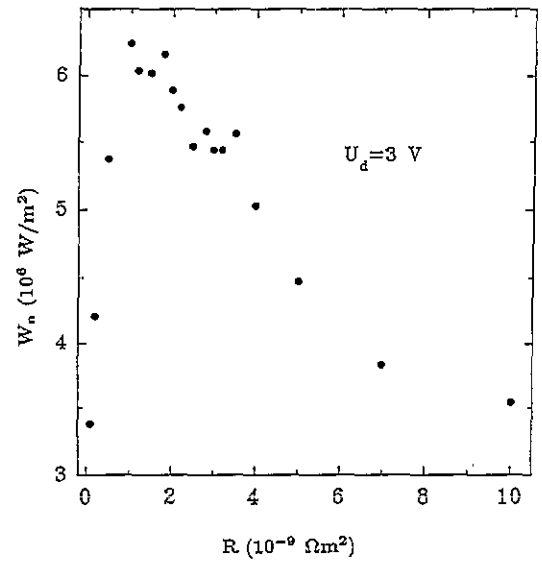


Figure 7. Total noise power integrated over the whole frequency range calculated by the MCP approach as a function of the load resistance.

curve the dependence of $(f_0, -R)$ obtained by the HD approach. To this purpose, $S_U(f)$ and $Z(f)$, calculated by the HD approach have been used to obtain the $P_n(f)$ spectra according to equation (3). We conclude that the frequency peak exhibited by $P_n(f)$ is the consequence of the spontaneous microwave generation in the near-linear regime (i.e. without the amplification feedback due to the external resonant circuit).

From the above analysis, we find that the peak in the noise power spectra at applied voltages above threshold is associated with the process of electron accumulation into layers due to the NDR. This is similar to the nonlinear process of microwave power generation when the diode is placed into an external resonant circuit, as may be proved by analysing the dependence on R of the total noise power integrated over the whole frequency range, $W_n = \int_0^\infty P_n(f) df$. Such a dependence, which is reported in figure 7, is typical of microwave generators operating in the resonant circuit. Here the maximum of W_n is achieved when R is in the range from 10^{-9} to $2 \times 10^{-9} \Omega \text{m}^2$. This result agrees well with the impedance spectrum (see figures 3 and 5) and with the results obtained from a simulation of microwave generation not presented here. The decrease of W_n with increasing R is explained by the damping of the high-frequency oscillations due to the load resistance, as is clearly seen in the noise spectrum (see curve 3 of figure 2).

For both cases, below and above the voltage threshold, the noise power spectra show a plateau in the low frequency range $f < 20$ GHz (see e.g. figure 2), which henceforth is called $P_n(0)$. Below the threshold, $P_n(0)$ increases with the voltage in correspondence with the low frequency impedance $\text{Re}[Z(0)]$. This is illustrated in figure 8, where the dependences of $P_n(0)$ and $\text{Re}[Z(0)]$ (both normalized to their values at $U_d = 0.04$ V) upon the diode bias are shown by the full circles and full curve respectively. Just above the threshold, $P_n(0)$ and $\text{Re}[Z(0)]$ change their slope. This

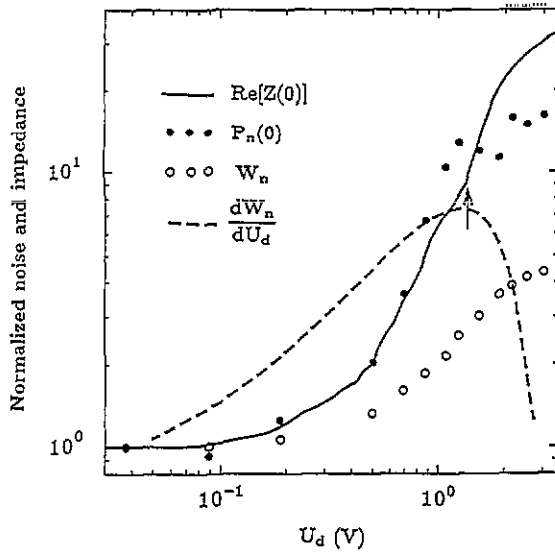


Figure 8. Zero-frequency impedance (full curve), low-frequency noise power (full circles), total noise power (open circles) and its derivative dW_n/dU_d (broken curve) as functions of the voltage applied to the diode. The arrow in the figure indicates the threshold voltage of the dynamic NDR.

can be explained by a redistribution in the frequency domain of the noise power spectrum, a redistribution that is associated with the onset of microwave power generation in the high frequency range. Indeed, the generation leads to a considerable enhancement of the noise power density in the frequency region where $\text{Re}[Z(f)]$ exhibits negative values. This yields a reduction of the low-frequency noise, if we assume that W_n has no significant variations near the threshold voltage. Such an explanation is in good agreement with the monotonic increase of W_n with U_d , as reported in figure 8 by the open circles. Nevertheless, above threshold the appearance of the generation influences the dependence of W_n on U_d too. Indeed, the behaviour of dW_n/dU_d , as reported in figure 8 by the broken curve, exhibits a maximum at the threshold voltage.

4. Conclusions

By performing a theoretical analysis of the noise spectra of submicron n^+nn^+ InP diodes we have proved that the calculation of these spectra provides useful information. In particular, we have determined the dynamic impedance and the upper frequency limit for microwave generation. From the calculation of the

frequency of the noise peak as a function of the load resistance one can obtain negative values of the real part of the small-signal impedance in the high frequency range of the spectrum. The full spectrum of the small-signal impedance can be recalculated by making use of an original procedure that requires at least three independent calculations of the noise power spectrum for the corresponding three different values of the load resistance. The threshold voltage for the appearance of a dynamic negative differential resistance has been determined by evaluating the noise power at low frequency as a function of the voltage applied to the diode.

Acknowledgments

This work is supported by a NATO collaborative research grant No 931360 and has been performed within the European Laboratory for Electronic Noise (ELEN) supported by the Commission of European Community through the contracts EKBXCT920047 and ERBCHICT920162. Partial support from the Ministero della Università e della Ricerca Scientifica e Tecnologica is gratefully acknowledged.

References

- [1] Nougier J P (ed) 1991 *III-V Microelectronics* (Amsterdam: Elsevier) p 183
- [2] Reggiani L, Kuhn T and Varani L 1992 *Appl. Phys. A* **54** 411
- [3] Cappy A 1988 *IEEE Trans. Microwave Theory Tech.* **36** 1
- [4] Filicori F, Ghione G and Naldi C U 1992 *IEEE Trans. Microwave Theory Tech.* **40** 1333
- [5] Zimmermann J and Constant E 1980 *Solid-State Electron.* **23** 915
- [6] Gružinskis V, Starikov E, Shiktorov P, Reggiani L, Saraniti M and Varani L 1993 *Simulation of Semiconductor Devices and Processes* vol 5, ed S Selberherr et al (Wien: Springer) p 333
- [7] Gružinskis V, Starikov E, Shiktorov P, Reggiani L, Saraniti M and Varani L 1993 *Semicond. Sci. Technol.* **8** 1283
- [8] Mitin V, Gružinskis V, Starikov E and Shiktorov P 1994 *J. Appl. Phys.* **75** 935
- [9] Gružinskis V, Starikov E, Shiktorov P, Reggiani L and Varani L 1994 *Phys. Rev. B* **49** at press
- [10] Gružinskis V, Starikov E, Shiktorov P, Reggiani L, Saraniti M and Varani L 1993 *Noise in Physical Systems and 1/f Fluctuations* ed P H Handel and A L Chung (New York: AIP) p 312